

CFD-based Underwater Formation Analysis for Multiple Amphibious Spherical Robots

Xihuan Hou^{1,2}, Shuxiang Guo^{1,2,3*}, Liwei Shi^{1,2*}, Huiming Xing^{1,2}, Yu Liu^{1,2}
Yao Hu^{1,2}, Debin Xia^{1,2}, Zan Li^{1,2}

¹Key Laboratory of Convergence Medical Engineering System and Healthcare Technology, The ministry of Industry and Information Technology, Beijing Institute of Technology

No.5, Zhongguancun South Street, Haidian District, Beijing 100081, China

²Key Laboratory of Biomimetic Robots and Systems, Ministry of Education, Beijing Institute of Technology

No.5, Zhongguancun South Street, Haidian District, Beijing 100081, China

³Faculty of Engineering, Kagawa University, 2217-20 Hayashi-cho, Takamatsu, Kagawa, Japan

houxihuan@bit.edu.cn, guoshuxiang@bit.edu.cn

*Corresponding author

Abstract—As limited sensing and working capability of a single robot, multiple robots cooperative accomplishing complex tasks in formation has been a popular topic in recent years. Energy efficiency is the premise and guarantee for underwater robot to complete a wide range of task, especially for the small and bionic amphibious spherical robots with limited energy. This paper analyzed three formation shapes in the view of underwater hydrodynamic drag aiming at decreasing the energy consumption of a multiple robots system. Numerical simulation based on Computational Fluid Dynamic (CFD) is adopted to compute the drag of each individual robot and entire systems. Simulation results show that triangular formation shape can decrease the total drag. When the serial and parallel formation are needed, the longitudinal distance and transverse distance should be short as soon as possible.

Index Terms—Amphibious spherical robot, Underwater formation, Computational fluid dynamic (CFD).

I. INTRODUCTION

with the increased interest in exploring activities of amphibious environment, amphibious robots with multiple sensors have been one of the tools to extend human hands. Such robots have been used for monitoring, detection of pollution [1], vision perception [2], and other tasks [3]–[5]. As a limited range of sensing and perception, solo robot can not accomplish complex task in a wide range of area [6]. Researches of multiple robots have been a focus in recent years. However, the cruise range and operation endurance of multiple robots is dictated by their finite energy source. In order to extend the endurance, minimizing the energy consumption of both individuals and the entire system is required. Some simple observations of crowded animals motion suggest that the drag of an individual may be reduced by certain formation configurations [7], examples such as, birds form an echelon formation for long distance migration [8], fish swimming in schools [9], dolphins in pods [10] and so on. The effect of human drafting distance on the drag coefficient in swimming was determined [11], which

highlighted that relative drag coefficient of the back swimmer was lower (about 56 percentage of the leading swimmer) for the smallest inter-swimmer distance (0.5 m).

Some studies have demonstrated that specific longitudinal and transverse offsets of multiples AUVs achieved energy consumption decreasing. Cooperation of AUV motion is simulated with CFD to observe the relationship between drag and longitudinal distance in the literature [12]. The tetrahedron shape of multiple AUVs formation has some influence factors on power efficiency, which is researched in the literature [13]. The influence of the propeller race on upstream and downstream self-propelled AUVs was investigated with the commercial RANS code ANSYS CFX [7]. Rattanasiri discussed the influence of the configuration's shape of multiple hulls in the vee and echelon formations [14].

Amphibious spherical robots are small bionic robots with much less power than AUVs [15]–[17]. In addition, the bionic driving mechanism of the robots, vector-jet propulsion, can cause turbulence and may have influence on the drag of surrounding other robots. To improve the endurance of multiple amphibious spherical robots system in the view of energy, longitudinal and transversal distance of some specific formation is essential. According to the behavior of fish swimming, three shapes of planar formation are selected as the analyzing objects of the paper, serial formation, parallel formation and triangular formation. Considering the computation efficiency, each formation shape is composed with minimum number of robots. Effects of longitudinal and transversal distance on Drag of individuals and the entire system are analyzed with the commercial computation software ANSYS CFX.

The rest of the paper is organized as follows. Section II depicts the model of multiple amphibious spherical robots. Numerical settings are detailed in Section III. Simulation results and discussions are described in Section IV. Finally,

Section V concludes this paper with an outline of future work.

II. MODEL OF MULTIPLE AMPHIBIOUS SPHERICAL ROBOTS FORMATION

A. An Amphibious Spherical Robot

Fig. 1 shows the amphibious spherical robot, which mainly consisted of a hemispherical upper hull, a circular middle plate, a legged water-jet composite driving mechanism, two quarter-spherical shells, a detachable battery cabin with 13,200 mAh, and sensors, such as pressure sensors, an inertial measurement unit (IMU), and a stereo camera [18]. The hemispherical part of the robot is consist of sealed cabin and adapting-buoyancy cabin. All electronic instruments are placed in the sealed cabin. The legged water-jet composite driving mechanism consists four same structure distributed surrounding the middle plate. The robot can achieve motions of forward, up-sink and rotating. The research of multiple robots formation configuration is based on the forward motion. Fig. 2 depicts the forward motion of the robot. The total length of the forward model is 57 cm and diameter of the circular middle plate is 30 cm.

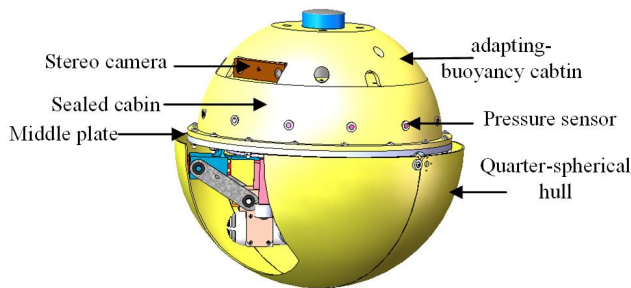


Fig. 1. Prototype of the amphibious spherical robot.

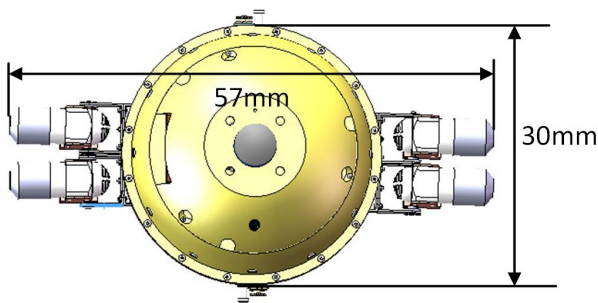


Fig. 2. Forward motion of the amphibious spherical robot.

B. Model of Multiple Robots Formation

Wake due to the water-jet propulsion of individual robot have influence on the surrounding flow that may affects the hydrodynamic drag of other robots. According to fish swimming school behaviors, serial formation, parallel formation and triangular formation, as three basic formation shapes,

are chose as the main analyzing objects. The Most simple model of the serial formation is consist of two robots, as shown in Fig.3. In the serial formation model, L is the total length of the robot, which is 57cm (as figure 2). D is the longitudinal distance between two robots. D is the only configure setting of serial formation. Fig. 4 depicts that two robots is considered in the model of parallel. In Fig. 4, D_2 is the transverse distance between two robots. Model of triangular formation containing three robots is shown in Fig. 5. A leader robot and two follower robots constitute a isosceles triangle. D_3 is the vertical distance from the leader robot to the line between two follower robots. Θ is the offset angle of the follower to the leader. Configuration of triangular formation contains two factors, D_3 and Θ .

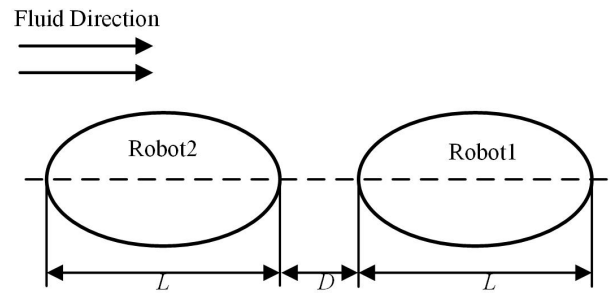


Fig. 3. Model of serial formation.

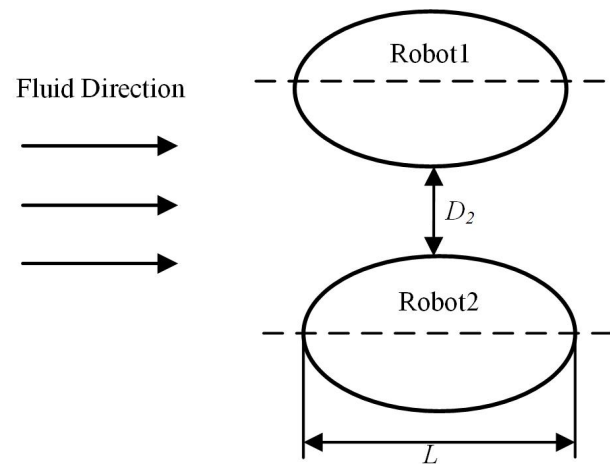


Fig. 4. Model of parallel formation.

III. NUMERICAL SETTINGS

In order to improve the endurance of the multiple amphibious spherical robots system from the point of energy, hydrodynamic drag of each individual robot and the entire robots should be small as soon as possible. The Hydrodynamic drag is given bt the equation1. At present, research of hydrodynamic drag based on CFD is relatively mature [19], [20]. The drag in this paper is calculated at the configuration

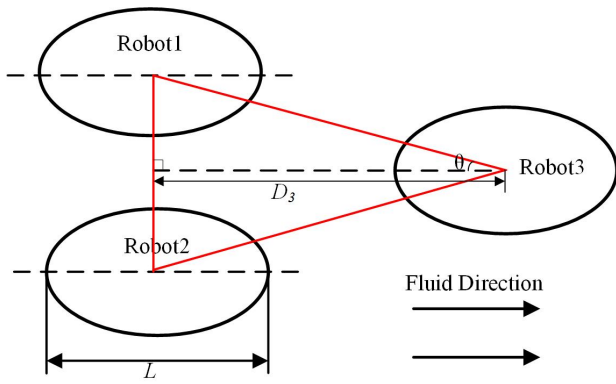


Fig. 5. Model of triangular formation.

parameters of different formations with the commercial software ANSYS CFX. Reasonable numerical settings is key to numerical simulation results. Main settings of the numerical computation are depict in detail.

A. Setting Computational Domain

In order to improve the computational efficiency, some inessential parts for the amphibious spherical robot are simplified. The simplified 3D model of the robot is shown in Fig. 6. The computational domain based on the simplified robot model should be large enough to avoid the influence of boundaries. According to the real experimental environment, shape of the computational domain is set as a cuboid. Size of the computation domain is set referring to the guidelines in ITTC 7.5-03-2-03 [21] and ITTC 7.5-03-3-01 [22]. The size of the cuboid in direction Z is $2.5D$, and D is the diameter of the robot. The other size in direction X and Y is determined by the formation model. The domain of the serial formation is described in Fig. 7. Size in direction X is $5L$, where L is the total length of the serial model. Size in direction Y is $3D$. Fig. 8 depicts the domain of the parallel formation, where the size in direction X is $5L$ and in direction Y is $3W$ (W is the total width of the formation model). Size settings of the triangular formation is same as parallel formation, as shown in Fig. 9.

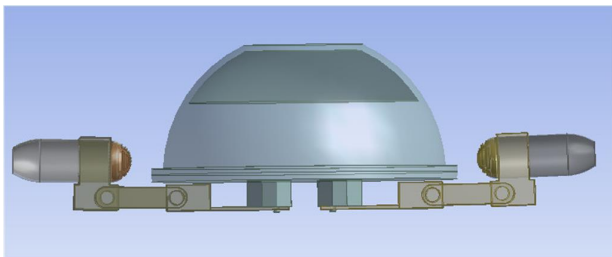


Fig. 6. Simplified amphibious spherical robot model.

B. Numerical Grids and Solver Settings

Size and amount of the domain mesh have a impact on the hydrodynamic computation. Large grids lead low precision,

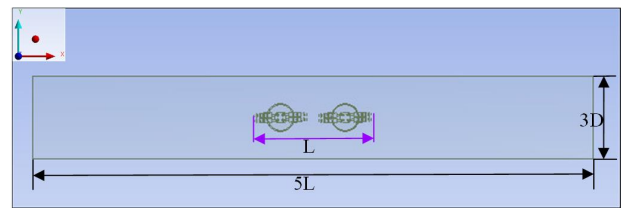


Fig. 7. Computational domain of the serial formation.

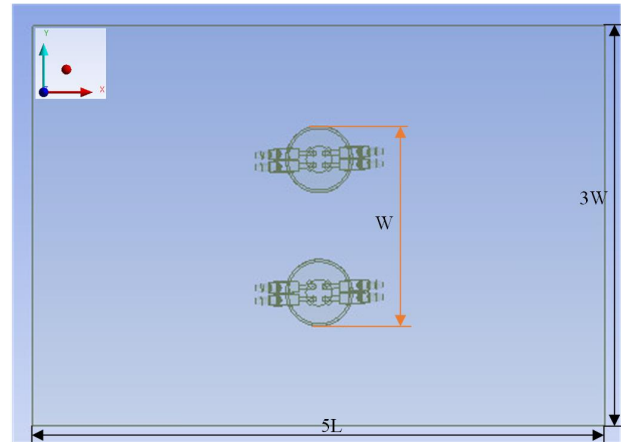


Fig. 8. Computational domain of the parallel formation.

while small grids lead large amount and high computing cost. The mesh of all domains are produced in the ANSYS-Mesh software. Finally, all the grids are smoothed and some particular grids are adjusted in ICEM [18]. Considering the paper space limited, only mesh of parallel formation is shown in Fig. 10.

The boundary conditions of the numerical simulation contains velocity-inlet and opening-outlet. The velocity of the inlet is set as 0.3 m/s . As the higher accuracy for hydrodynamic simulation, the shear stress transport (SST) turbulence model is adopted to compute the hydrodynamic results. In addition, when the average residuals of RMS (root mean square) drop to 1×10^{-4} , the computational results are seen as convergence.

IV. RESULTS AND DISCUSSION

Hydrodynamic drags of each individual robot and multiple system are calculated based on above numerical settings. For multiple system owning N robots, non-dimensional parameters are defined as the following equations to observe drags changes.

$$C(1) = \frac{Drag_1 - Drag}{Drag} \quad (1)$$

$$C(2) = \frac{Drag_2 - Drag}{Drag} \quad (2)$$

$$C(N) = \frac{Drag_N - Drag}{Drag} \quad (3)$$

$$C(T) = \frac{Drag_1 + Drag_2 + \dots + Drag_N - NDrag}{NDrag} \quad (4)$$

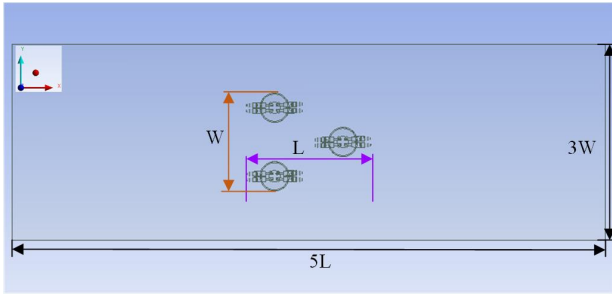


Fig. 9. Computational domain of the triangular formation.

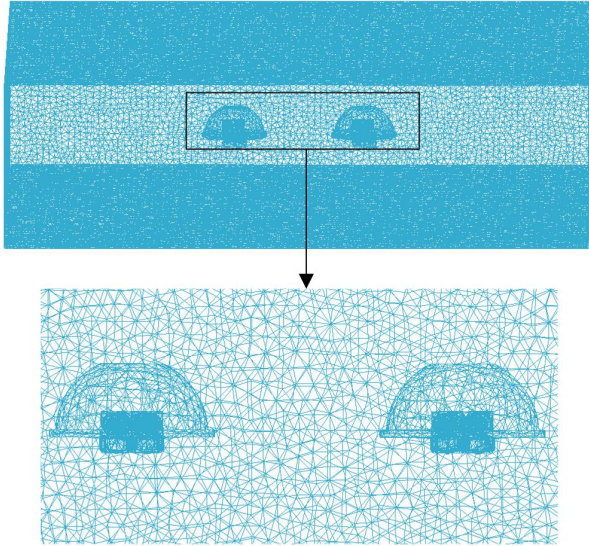


Fig. 10. Mesh of the parallel formation.

$Drag_N$ is the hydrodynamic drag of the N-th robot in the multiple robots formation system. $Drag$ is the drag of an individual robot without formation. Varies of above defined parameters with longitudinal and transverse distance will be analyzed in the following.

A. Results of Serial Formation

In the serial formation system, there are two robots. As there is acoustic-based communication between two robots, the longitudinal distance of two robots only varies from 0 to 0.9m. Fig. 11 shows that the trend of non-dimension parameters in this interval. $C(1)$ is the drag changes of the leader robot. $C(2)$ is drag changes of the follower robot. $C(T)$ is the drag of the entire robots. It is found that drag of the leader robot is larger than that of without formation and drag of the follower robot is almost same with that of without formation. This trend is consist with the phenomenon of dolphins in pods. With the distance increasing, the drags of leader and follower robot converge towards that without formation. The total drag of the formation system is little larger than that of without formation at the outset. With the distance increasing, the total drag rise gradually. Smaller longitudinal distance of the serial formation can reduce the

drag. The smaller the distance is, the smaller the hydrodynamic resistance is. Therefore, when the serial formation is needed in the multiple robots system, the distance between two adjacent robots should be smaller as soon as possible. Above trend can extend the multiple robots system owning more robots. To observe the distribution of flow intuitively, velocity contours and pressure contours as the distance is 0.23m are visualized in Fig. 12 and Fig. 13, respectively.

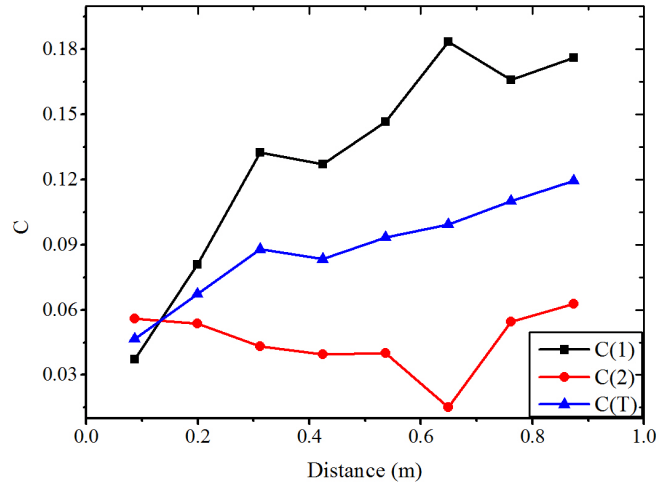


Fig. 11. Drag of the serial formation.

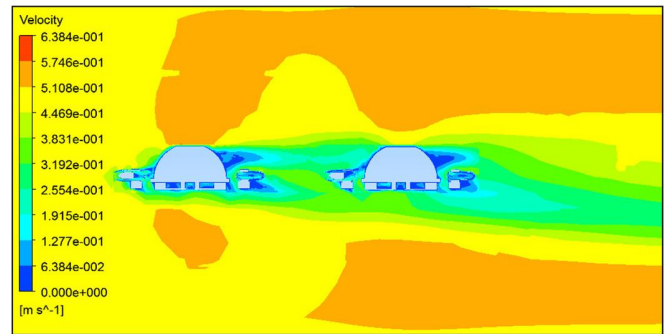


Fig. 12. Drag of the serial formation.

B. Results of parallel Formation

In the parallel formation system, there are also two robots. The transverse distance of two robots varies from 0 to 0.6m. Changes of the non-dimension parameters with the transverse distance are described in Fig. 14. Drag of each robot in parallel formation is almost same and is little larger than that of without formation. Compared to serial formation, this formation shape can not reduce the entire drag and the distance have less influence on drag of each robot and entire system. If there is need of this shape formation, the distance of two robots should be short as soon as possible. To visualize the flow distribution in parallel formation, Fig.15(a) and (b) lists the velocity contours and pressure contours when the distance is 0.4m.

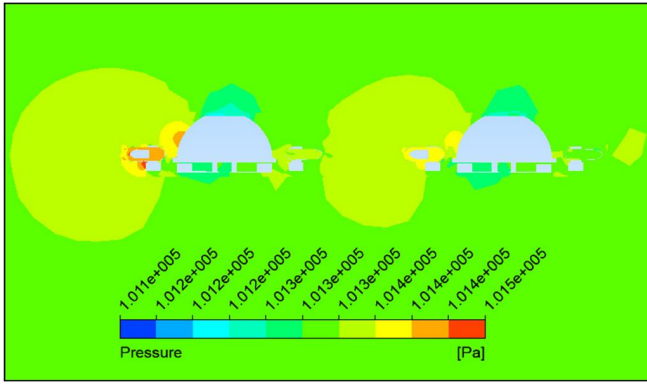


Fig. 13. Drag of the serial formation.

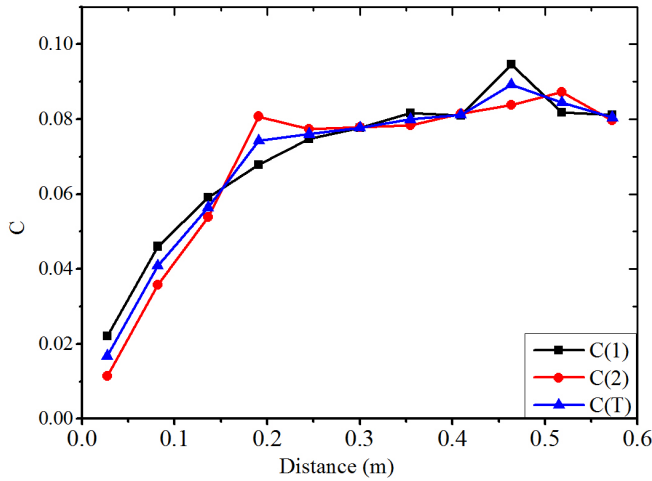


Fig. 14. Drag of the parallel formation.

C. Results of Triangular Formation

In the triangular formation hydrodynamic simulation system, there are three robots. The transverse distance of two follower robots and the vertical longitudinal distance between the leader and follower are considered as two factors impact on the individual and entire drag as shown in Fig. 5 in section II. The transverse distance and the vertical longitudinal both vary in the range of 0 – 0.6m. Method of Controlling Variables is adopted to research the transverse and longitudinal distance influence on hydrodynamic drag. Fig. 16 depicts the changes of drags with the vertical longitudinal distance when the transverse distance is controlled at 0.6m, respectively. Drag of the leader robot is a little smaller than that of without formation. Drags of two follower robots are almost same and a little larger than that without formation. As the vertical longitudinal distance increasing, drag of each robot has little changes. Compared to above two shapes, the total drag of this formation configuration decreases, which illustrates that this formation shape can reduce the entire drag and then decrease the energy consumption. Fig. 17 describes changes of the drag with the transverse distance when the vertical longitudinal distance is controlled at 0.3m. It is found that

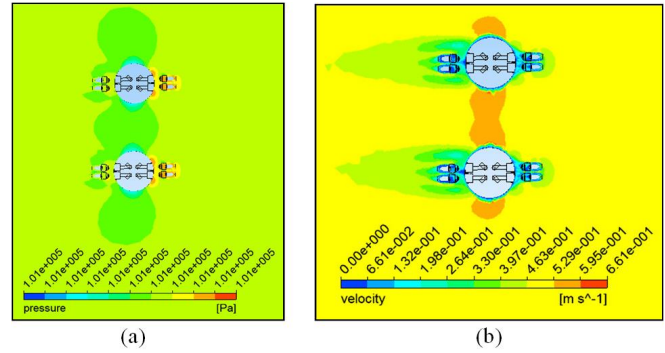


Fig. 15. Pressure and velocity contours when the distance is 0.4m. (a) Pressure contour. (b) Velocity contour.

drags of two follower robots reach the minimum value when the transverse distance is 0.3m. And the total drag of the entire system is also minimal at this set. When the longitudinal distance is 0.3m, pressure contours with transverse distance 0.25m and 0.6m are shown in Fig. 18(a) and (b), and velocity contours are depicted in Fig. 19(a) and (b), respectively.

According to all analysis of triangular formation, it is illustrated that when transverse and longitudinal distance are set as 0.3m, the multi-robot system suffers minimum resistance and gets the highest energy efficiency.

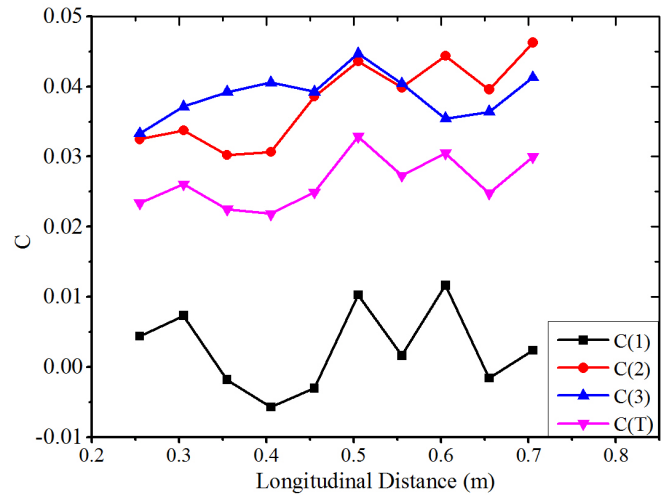


Fig. 16. Drag of the triangular formation when transverse distance is 0.6m.

V. CONCLUSION

For the small and bionic amphibious spherical robots, energy is very limited. In order to improve the endurance in underwater environment, it is essential to design a suitable formation shape for multiple robots system. Reducing the hydrodynamic drag can decrease the energy consumption. Therefore, hydrodynamic simulation-based drags of each robot and entire system of three formation shapes were researched. According to analysis of drags in three formation shapes, the serial and parallel formation shape can not reduce the drag of the entire system, while triangular formation

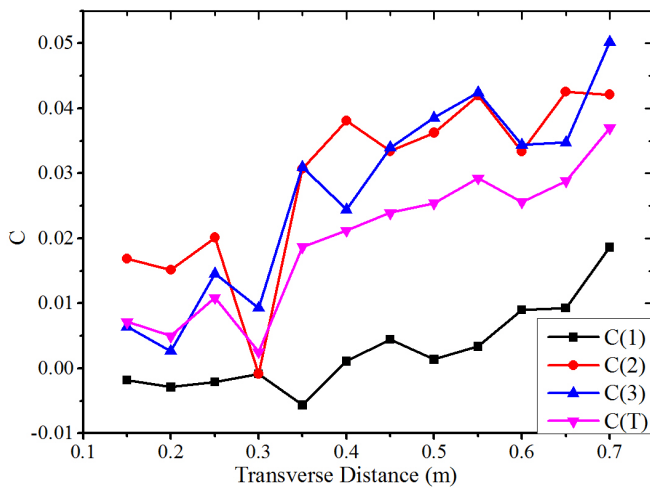


Fig. 17. Drag of the triangular formation when longitudinal distance is 0.3m.

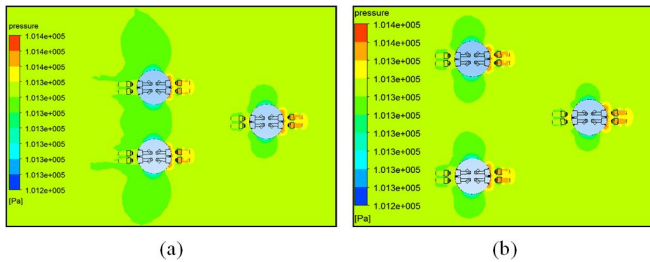


Fig. 18. Pressure contours of the triangular formation at different formation configurations.(a) Pressure contour of 0.25m transverse distance.(b) Pressure contour of 0.6m transverse distance

shape can decrease the drags of follower robots and the entire system. If there is no requirements, multiple robots had better keep a triangular formation keeping the transverse and longitudinal distance at 0.3m. If the serial and parallel formation shape is needed, the longitudinal and transverse distance should be short as soon as possible to guarantee relatively small drags.

VI. ACKNOWLEDGMENT

This work was partly supported by National High Tech. Research and Development Program of China (No.2015AA043202), the National Natural Science Foundation of China (61773064, 61503028), the National Key Research and Development Program of China (No. 2017YFB1304401), and Graduate Technological Innovation Project of Beijing Institute of Technology (2018CX10022).

REFERENCES

- [1] H. Xing, S. Guo, L. Shi, Y. He, S. Su, Z. Chen, "Hybrid Locomotion Evaluation for a Novel Amphibious Spherical Robot," *Applied Sciences*, vol.8, no.2, doi:10.3390/app8020156, 2018.
- [2] H. Xing, L. Shi, K. Tang, S. Guo, X. Hou, Y. Liu, H. Liu, Y. Hu. "Robust RGB-D Camera and IMU Fusion-based Cooperative and Relative Close-range Localization for Multiple Turtle-inspired Amphibious Spherical Robots," *Journal of Bionic Engineering*, vol.16, no.3, pp.442-454, 2019.
- [3] Y. He, S. Guo, L. Shi, "Preliminary Mechanical Analysis of an Improved Amphibious Spherical Father Robot," *Microsyst. Technol.*, vol.22, pp.2051-2066, doi:10.1007/s00542-015-2504-9, 2016.

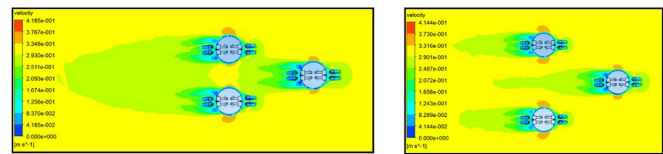


Fig. 19. Velocity contours of the triangular formation at different formation configurations.(a) Velocity contour of 0.25m transverse distance.(b) Velocity contour of 0.6m transverse distance

- [4] S. Guo, S.Pan, X. Li, L. Shi, "A System on Chip-based Real-time Tracking System for Amphibious Spherical Robots," *Int. J. Adv. Robot. Syst.*, vol.14, no.4, pp.1-19, 2017.
- [5] S. Guo, S.Pan, L. Shi, "Visual Detection and Tracking System for an Amphibious Spherical Robot," *Sensors*, vol.17, no.4, doi:10.3390/s17040870, 2017.
- [6] Y. He, L. Zhu, G. Sun, J. Qiao, S. Guo, "Underwater motion characteristics evaluation of multi amphibious spherical robots", *Microsystem Technologies*, Vol.25, No.2, pp.499-508, 2019.
- [7] P. Rattanasiri, P. A. Wilson, A. B. Phillips, "Numerical investigation of a pair of self-propelled AUVs operating in tandem," *Ocean Engineering*, vol.100, pp.126-137, doi:10.1016/j.oceaneng.2015.04.031, 2015.
- [8] M. Andersson, J. Wallander, "Kin selection and reciprocity in flight formation?" *Behavioral Ecology*, vol.15, no.1, pp.158-162, 2004.
- [9] B. Hanrahan, F. Juanes, "Estimating the number of fish in Atlantic Blue fin Tuna schools using models derived from captive school observations," *Fish. Bull.*, vol.99 no.3, pp.420-431, 2001.
- [10] D. Weihs, "The hydrodynamics of dolphin drafting," *Journal of Biology*, vol.3, no.2, pp.8, 2004.
- [11] A.J. Silva, A. Rouboa, A. Moreira, V.M. Reis, F.Alves, J.P. Vilas-Boas, D.A. Marinho, "Analysis of drafting effects in swimming using computational fluid dynamics" *Journal of Sports Science and Medicine*, vol.7, no.1, pp.60-66, 2008.
- [12] M. Husaini, "CFD simulation of cooperative AUV motion," *Indian Journal of Geo-Marine Sciences*, vol.38, no.3, pp.346-351, 2009.
- [13] N. Burlutskiy, T. Yaniss, "Power efficient formation configuration for centralized leader-follower AUVs control," *Journal of Marine Science and Technology*, vol.17, no.3, pp.315-329, 2012.
- [14] P. Rattanasiri, P. A. Wilson, A. B. Phillips, "Numerical investigation of a fleet of towed AUVs," *Ocean Engineering*, vol.80, pp.25-35, doi:10.1016/j.oceaneng.2014.02.001, 2014.
- [15] L. Zheng, S. Guo, S. Gu, "The communication and stability evaluation of amphibious spherical robots", *Microsystem Technologies*, Vol.24, pp.1-12, doi:10.1007/s00542-018-4223-5, 2018.
- [16] M. Li, S. Guo, H. Hirata, H. Ishihara, "A Roller-skating/Walking Mode-based Amphibious Robot" *Robotics and Computer Integrated Manufacturing*, Vol.44, pp.17-29, doi:10.1016/j.rcim.2016.06.005, 2016.
- [17] M. Li, S. Guo, Jin Guo, H. Hirata, H. Ishihara, "Development of a biomimetic underwater microrobot for a father-son robot system" *Microsystem Technologies*, Vol.23, No.4, pp.1-13, 2016
- [18] X.Hou, S. Guo, L. Shi, H. Xing, Y. Liu, H. Liu, Y. Hu, D. Xia, Z. Li, "Hydrodynamic Analysis-Based Modeling and Experimental Verification of a New Water-Jet Thruster for an Amphibious Spherical Robot," *Sensors*, vol.19, no.259, doi:10.3390/s19020259, 2019.
- [19] T.H. Joung, H.S. Choi, S.K. Jung, K. Sammut, F.P.He, "Verification of CFD Analysis Methods for Predicting the Drag Force and Thrust Power of an Underwater Disk Robot," *Int. J. Nav. Archit. Ocean Eng.*, vol.6, no.2, pp.269-281, 2014.
- [20] X. Hou, S. Guo, L. Shi, H. Xing, S. Su, Z. Chen, et al., "Hydrodynamic Analysis of a Novel Thruster for Amphibious Sphere Robots," in *Proceedings of 2018 IEEE International Conference on Mechatronics and Automation*, August 5-8, Changchun, China, pp.1603-1608, 2018.
- [21] ITTC-Recommended Procedures and Guidelines, "Practical Guidelines for Ship CFD Application 7.5-03-2-03," in *Proceedings of the 27th International Towing Tank Conference (ITTC)*, Copenhagen, Denmark, Sep.2014.
- [22] ITTC-Recommended Procedures and Guidelines, "Practical Guidelines for Ship Self-Propulsion CFD 7.5-03-03-01," in *Proceedings of the 27th International Towing Tank Conference (ITTC)*, Copenhagen, Denmark, Sep.2014.